Original Article
https://doi.org/10.5115/acb.2019.52.1.48
pISSN 2093-3665 eISSN 2093-3673
Anatomy & Cell Biology acb

Nerve distribution in myocardium including the atrial and ventricular septa in late stage human fetuses

Kwang Ho Cho[1], Ji Hyun Kim[2], Gen Murakami[3], Hiroshi Abe[4], José Francisco Rodríguez-Vázquez[5], Ok Hee Chai[2]

[1]Department of Neurology, Wonkwang University School of Medicine and Hospital, Institute of Wonkwang Medical Science, Iksan, [2]Department of Anatomy and Institute of Medical Sciences, Chonbuk National University Medical School, Jeonju, Korea, [3]Division of Internal Medicine, Asuka Hospital, Sapporo, [4]Department of Anatomy, Akita University School of Medicine, Akita, Japan, [5]Department of Anatomy and Human Embryology, Institute of Embryology, Faculty of Medicine, Complutense University, Madrid, Spain

Abstract: Few information had been reported on deep intracardiac nerves in the myocardium of late human fetuses such as nerves at the atrial-pulmonary vein junction and in the atrial and ventricular septa. We examined histological sections of the heart obtained from 12 human fetuses at 25–33 weeks. A high density of intracardiac nerves was evident around the mitral valve annulus in contrast to few nerves around the tricuspid annulus. To the crux at the atrioventricular sulcus, the degenerating left common cardinal vein brought abundant nerve bundles coming from cardiac nerves descending along the anterior aspect of the pulmonary trunk. Likewise, nerve bundles in the left atrial nerve fold came from cardiac nerves between the ascending aorta and pulmonary artery. Conversely, another nerves from the venous pole to the atrium seemed to be much limited in number. Moreover, the primary atrial septum contained much fewer nerves than the secondary septum. Therefore, nerve density in the atrial wall varied considerably between sites. As ventricular muscles were degenerated from the luminal side for sculpturing of papillary muscles and trabeculae, deep nerves became exposed to the ventricular endothelium. Likewise, as pectineal muscles were sculptured, nerves were exposed in the atrial endothelium. Consequently, a myocardial assembly or sculpture seemed to be associated with degeneration and reconstruction of early-developed nerves. A failure in reconstruction during further expansion of the left atrium might be connected with an individual variation in anatomical substrates of atrial fibrillation.

Key words: Heart, Epicardiac nerves, Venous pole, Mitral valve, Atrial septum, Human fetus

Received August 1, 2018; Revised August 23, 2018; Accepted October 12, 2018

Introduction

An entire view of human intracardiac nerves seemed to be first provided by Pauza et al. [1] who used an excellent technique of whole-mount histochemistry of acetylcholinesterase for human fetal hearts, they demonstrated that (1) epicardiac nerves provide seven subplexuses and (2) more than half ganglion cells are present at the dorsal and dorsolateral surfaces of the left atrium. They also ensured a specifically concentrated nerve bundles in a fold separating the entrance of the left superior pulmonary vein from the left atria, i.e., the so-called

Corresponding author:
Ji Hyun Kim
Department of Anatomy, Chonbuk National University Medical School, 20 Geonji-ro, Deokjin-gu, Jeonju 54907, Korea
Tel: +82-63-270-3097, Fax: +82-63-274-9880, E-mail: 407kk@hanmail.net
Gen Murakami's current affiliation: Division of Internal Medicine, Jikoukai Clinic for Home Visit, Sapporo, Japan

left atrial nerve fold. This fold was first reported by Worobiew [2] and Gardner and O'Rahilly [3] later ensured the presence. This fold seems to correspond to the future atrial-pulmonary vein junction, the latter of which is likely to contain a histopathological substrate of chronic atrial fibrillation [4-7]. In addition to whole-mount studies, several histological and immunohistochemical studies had been conducted using sections of human adult hearts, not of fetuses [8-12]. In these reports, Marron et al. [8] was characterized by detailed descriptions of nerve terminal morphologies but, to our regret, there was no information about the atrial and ventricular septum.

According to our experience [13], the whole-mount histochemistry has a disadvantage that, in contrast to surface nerves, nerves embedded deeply in a connective tissue are not clearly demonstrated or even not stained because of limited infiltration of substrates for reaction. Likewise, a nerve running through a matured muscle is also difficult to demonstrate because of difficult transillumination through the dark

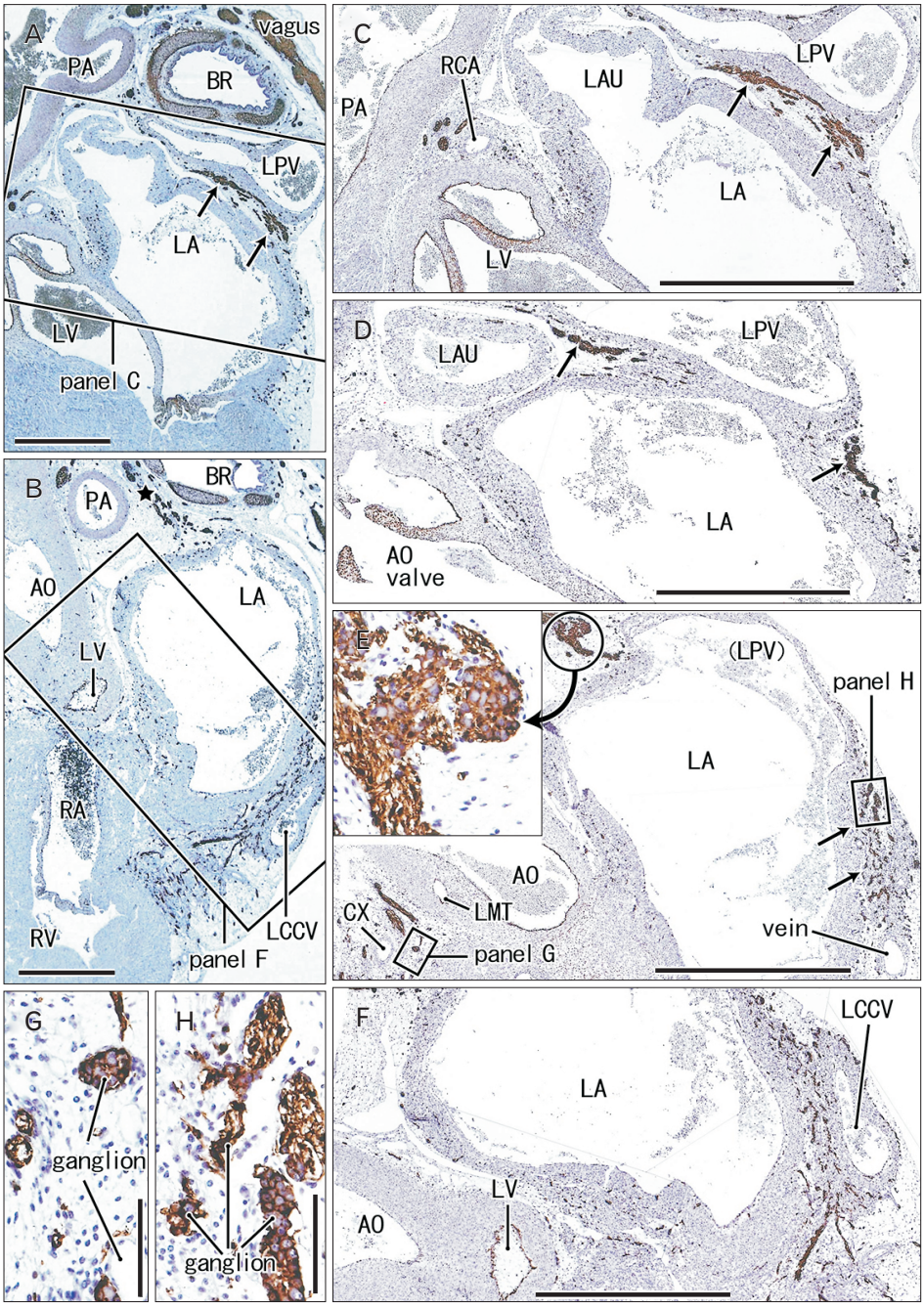

Fig. 1. Nerves descending between the left atrium (LA) and pulmonary vein to a site along the left common cardinal vein. 25 weeks. Sagittal sections. Immunostaining of S100 protein. Incomplete square in panel A (or B) indicates an area of panel C (or F) at the higher magnification. Ganglia in panel E are shown in panels G and H as well as in an insert at the center of this figure. Panels D and E display intermediate planes between panels C and F. The left pulmonary vein (LPV) drains into the LA in a plane between panels D and E. Abundant nerves around the left common cardinal vein (LCCV in B and F) comes from a superior site (star in B) between the left primary bronchus (BR) and pulmonary artery (PA) via a narrow space between the LPV and LA (arrows in panels A, C–E). AO, aorta; CX, circumflex branch of the left coronary artery; LAU, left auricle; LMT, main trunk of the left coronary artery; LV, left ventricle; RA, right atrium; RCA, right coronary artery; RV, right ventricle; Vagus, left vagus nerve. Scale bars=5 mm (A, B), 1 mm (C–F), 0.1 mm (G, H).

https://doi.org/10.5115/acb.2019.52.1.48

colored tissue. Thus, even in beautiful photographic by Pauza et al. [1], nerves in and through the ventricular myocardium were not demonstrated. Moreover, histological studies using human fetuses had focused on extrinsic innervation to the sinoatrial and atrioventricular nodes [3, 14]. Therefore, especially in the late stage fetuses with thick and matured cardiac muscles, there was no or few morphological information on (1) nerves around the atrioventricular orifices and and (2) nerves running through the ventricular wall and septum. The late stage fetus has also an advantage that the atrial-pulmonary vein junction is not yet established in association with a widely opened oval foramen. S100 protein was a neurospecific protein. This protein was generally considered to be a component in the glial and Schwann cells of peripheral nervous system [15]. Consequently, using histological sections with S100 protein immunohistochemistry, the aim of this study was to examine intracardiac nerve configuration in the late stage fetuses.

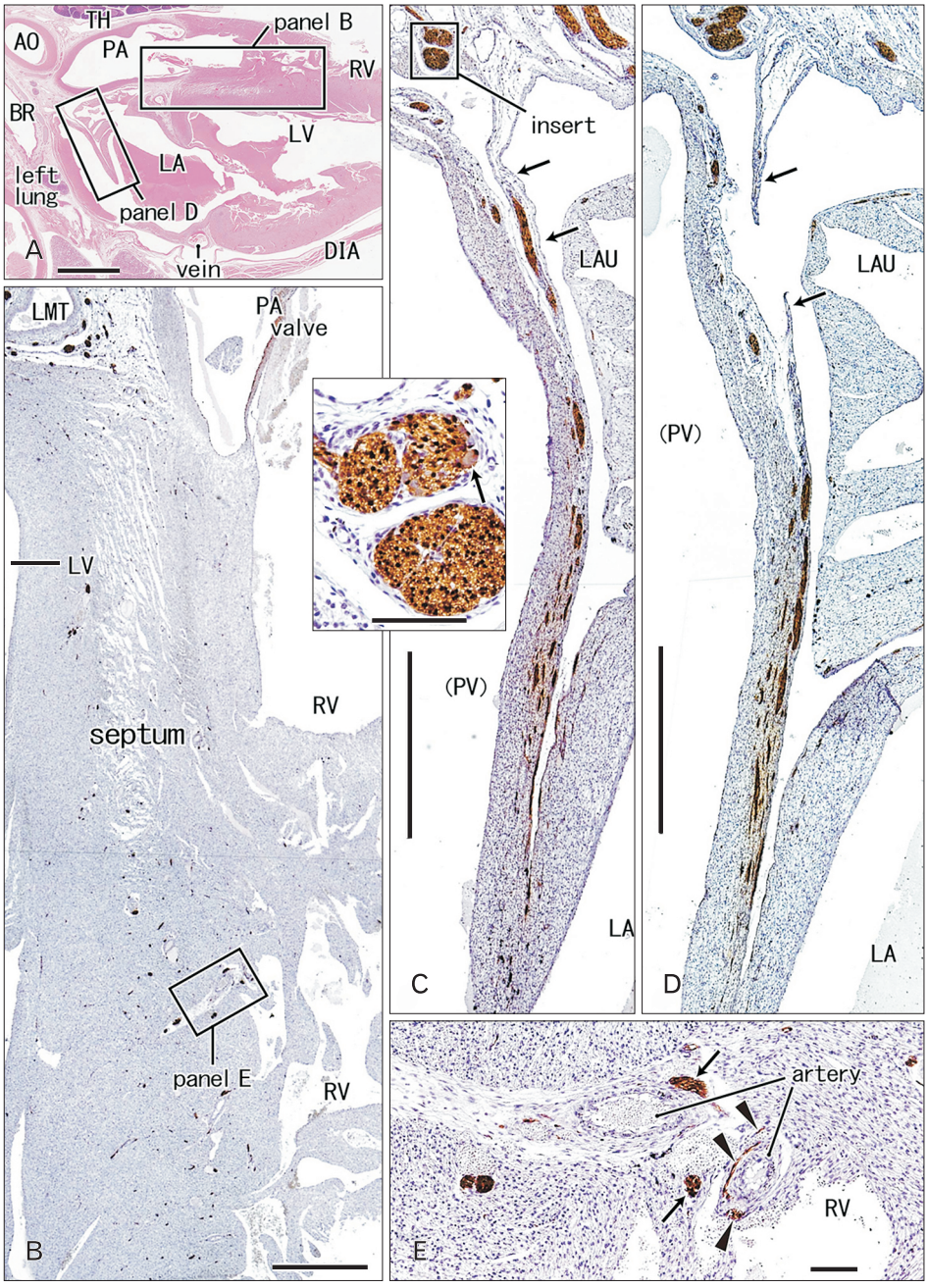

Fig. 2. Nerves and ganglia in the left atrial nerve fold and interventricular septum of the heart. 26 weeks. Sagittal sections through the outflow tract of the right ventricle (RV) and the interventricular septum. Hematoxylin and eosin staining (A) and immunostaining of S100 protein (B–E). Squares in panel A are shown in panels B and D at the higher magnification. Panel B shows abundant thin nerves in the interventricular septum: parts of muscular nerves (arrows in E) as well as nerve nets around arteries (arrowheads in E) are exposed to the expanding ventricular endothelium. Panel D as well as panel C (a plane 1 mm left side of D) exhibits the left atrial nerve fold: most of the nerve contents run through the future wall of the pulmonary vein (PV) and they come through a pericardial fold (arrows). An insert between panels B and C displays a ganglion cell (arrow) at the base of the nerve fold. AO, aorta; BR, bronchus; DIA, diaphragm; LA, left atrium; LAU, left auricle; LMT, left main trunk of the coronary artery; LV, left ventricle; PA, pulmonary artery; TH, thymus. Scale bars=5 mm (A), 1 mm (B–D), 0.1 mm (E, insert between B and C).

Materials and Methods

This study was performed in accordance with the provisions of the Declaration of Helsinki 1995 (as revised in 2013). We used frontal or sagittal sections of 12 masses of thoracic viscera obtained from 12 human fetuses at 25–33 weeks (crown-rump length, 200–280 mm). These fetuses were parts of a collection in Department of Anatomy, Akita University, Akita, Japan. They were donated by their families to the department during 1975–1985 and preserved in 10% w/w neutral formalin solution for more than 30 years. The available data was limited to the date of donation and the gestational weeks, but we did not find a document saying the family name, the name of obstetricians or hospital and the reason of

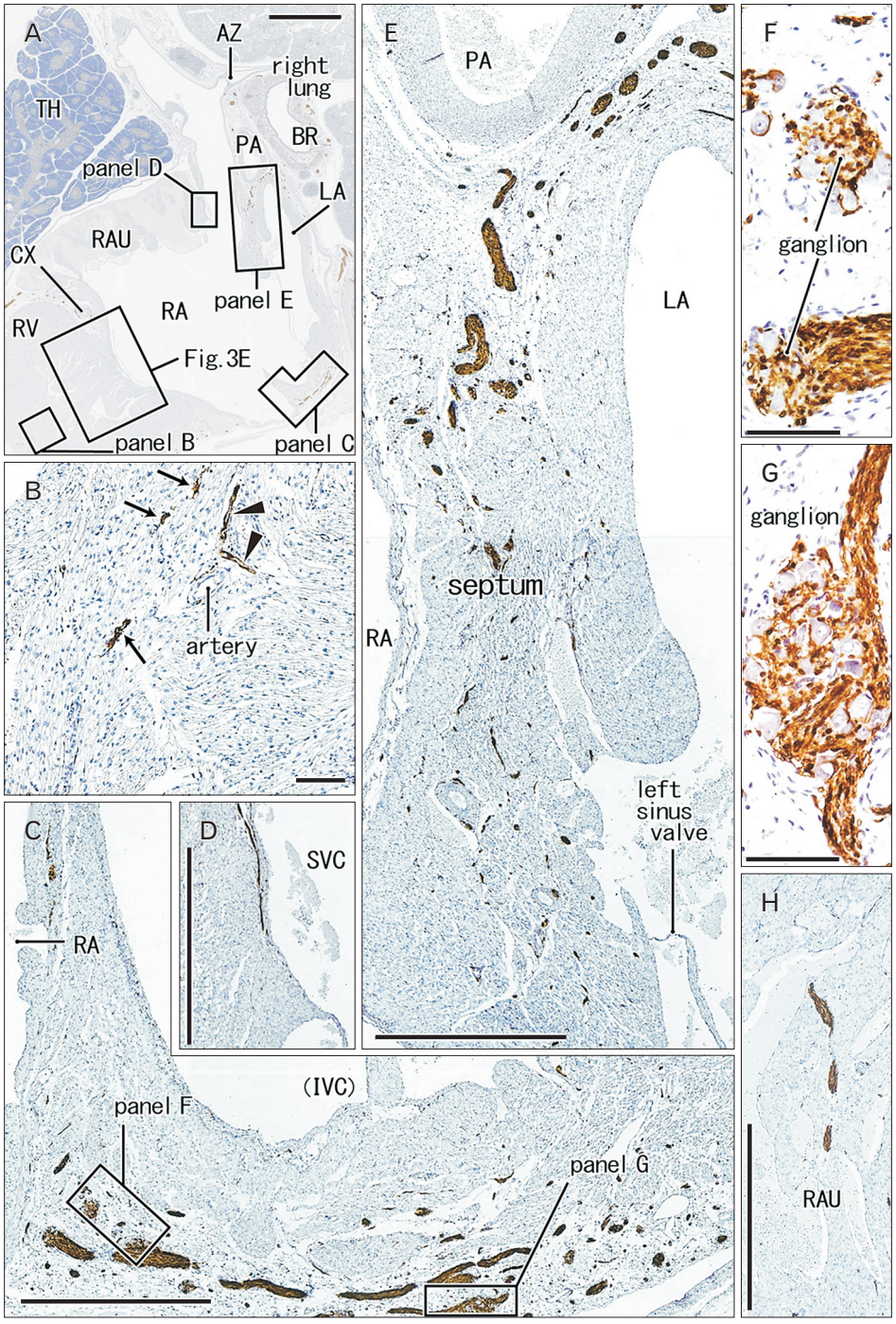

Fig. 3. Nerves and ganglia in the right ventricle and atrium of the heart. 31 weeks. Sagittal sections. Immunostaining of S100 protein. Squares in panel A are shown in panels B–E as well as Fig. 3E at the higher magnification. Panel B displays muscular nerves (arrows) and nerve nets along an artery (arrowheads) in the right ventricular wall. Panel C exhibits the right atrial wall near the orifice of the inferior vena cava (IVC): the ganglia are shown in panels F and G at the higher magnification. Panel D displays a nerve along the endothelium of the superior vena cava (SVC). Panel E shows nerves in the interatrial septum near the orifice of the pulmonary vein. Panel H, a plane 3 mm right of the other panels, exhibits a thick nerve passing through the right auricle (RAU). AZ, azygos vein; BR, bronchus; LA, left atrium; PA, pulmonary artery; RA, right atrium; RV, right ventricle; TH, thymus. Scale bars=5 mm (A), 0.1 mm (B, F, G), 1 mm (C–E, H).

https://doi.org/10.5115/acb.2019.52.1.48

abortion. The use for research was approved by the university ethics committee in Akita (No. 1428).

We prepared 12 paraffin blocks containing the whole heart as well as parts of the lung, thymus and diaphragm. From each of the blocks, we prepared 200-300 semiserial sections covering the entire heart (5-μm in thickness; 50-μm interval). One of every 5–10 sections were used for immunohistochemistry of S100 protein, while the others were used for stained with hematoxylin and eosin. The primary antibodies used were and a rabbit polyclonal anti-human S100 protein or S100 (dilution 1:100, Dako N1573, Dako, Glostrup, Denmark). After incubation for 30 minutes in Histofine Simple Stain Max-PO (Nichirei, Tokyo, Japan) for the diaminobenzidine (DAB) reaction with horseradish peroxidase, dark brown coloration (DAB reaction) were obtained. Sections stained using the DAB method were counterstained with hematoxylin. Observations and taking photographs were usually performed with Nikon Eclipse 80, but photos at ultra-low magnification (objective lens less than ×2) were taken using a high-grade flat scanner with translucent illumination (Epson scanner GTX970, Java, indonesia).

Results

Intracardiac nerves and ganglia are demonstrated (1) at and along the atrial wall (Figs. 1–4) including the left atrial nerve fold (Fig. 2C, D) and the atrial septa (Figs. 3E, 4C–F), (2) in the ventricular wall including the ventricular septa and

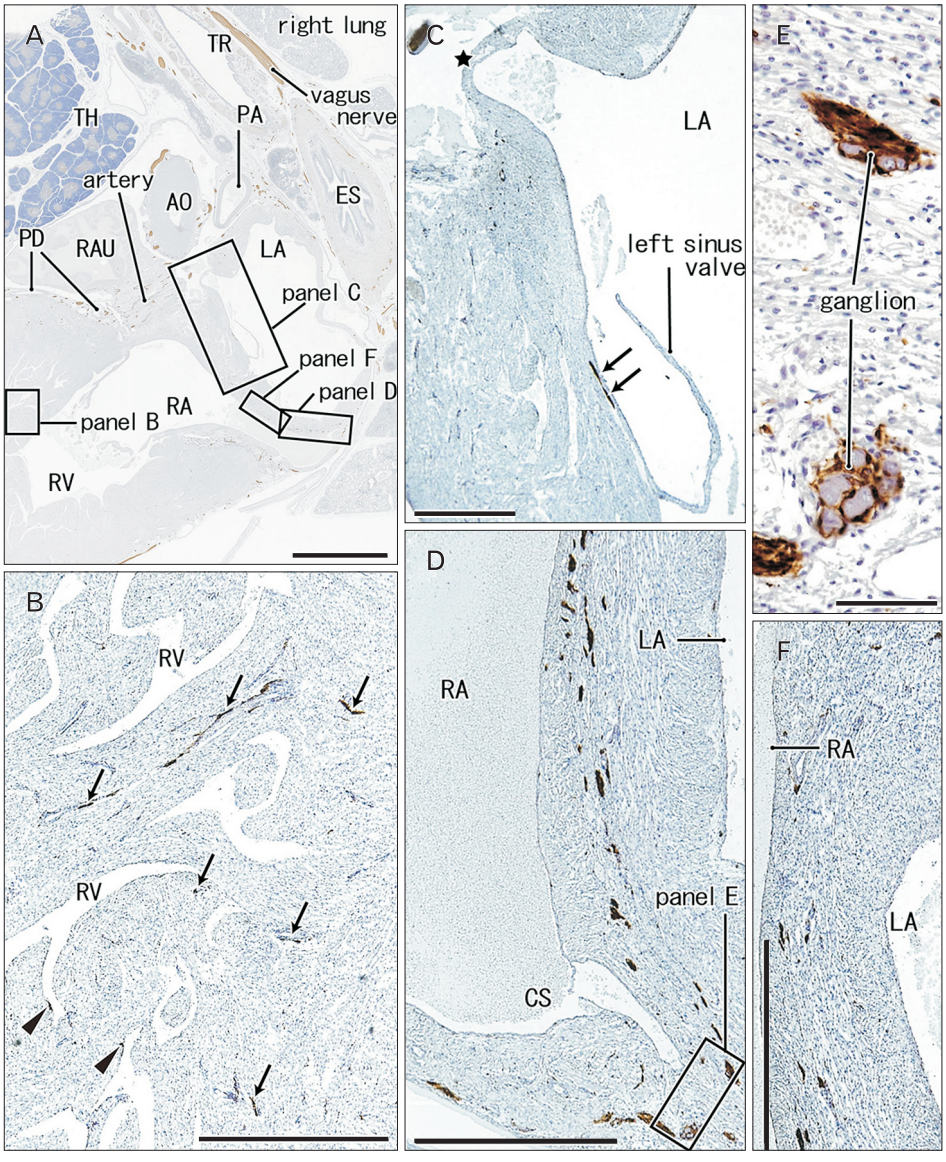

Fig. 4. Nerves and ganglia in the interatrial septum and right ventricular wall. 31 weeks. A specimen same as in Fig. 5. Sagittal sections 3 mm medial or left side of Fig. 4. Immunostaining of S100 protein. Squares in panel A are shown in panels B–D and F at the higher magnification. Panel B displays nerves (arrows and arrowheads) in the right ventricular wall: some of them (arrowheads) are exposed to the ventricular endothelium. Panel C exhibits the upper part of the interatrial wall, while panels D and F the lower part. Panel C contains a nerve along the endocardium (arrows) as well as an orifice of a minor cardiac vein draining into left atrium (star). Ganglia near the cavernous sinus (CS) are shown in panel E at the higher magnification. AO, aorta; ES, esophagus; LA, left atrium; PA, pulmonary artery; PD, posterior descending branch of the right coronary artery; RA, right atrium; RAU, right auricle; RV, right ventricle; TH, thymus; TR, trachea. Scale bars=5 mm (A), 1 mm (B–D, F), 0.1 mm (E).

annuluses of the mitral and tricuspid valves (Figs. 2B–E, 3B, 4B, 5) and (3) in the atrioventricular sulcus and at the base of great arteries (Figs. 1A, B, 6). Each of the figures is prepared for a single fetus except for Figs. 3 and 4 those display the primary and secondary atrial septa (septum primum and septum secundum) of the same specimen.

Ganglion cell bodies were round or oval and identified as negative areas in S100 immunohistochemistry. They ranged from 10 to 30 μm in diameter and the size was smaller in the earlier or smaller specimens, e.g., Fig. 1 (25 weeks) vs. Fig. 6 (30 weeks). Ganglion cell clusters were distributed (1) along the atrioventricular sulcus especially near the crux (Figs. 1E, 3C, 4D, 6B), (2) along the left main trunk of the left coronary artery (Figs. 1E, 5C, 6B), (3) at the origin of the right coronary artery (Fig. 1C), and (4) in front of the pulmonary arterial trunk (Fig. 6D). These ganglionated nerve plexuses corresponded to the left and right coronary subplexuses of Pauza et al. [1]. When roughly estimated using present semiserial

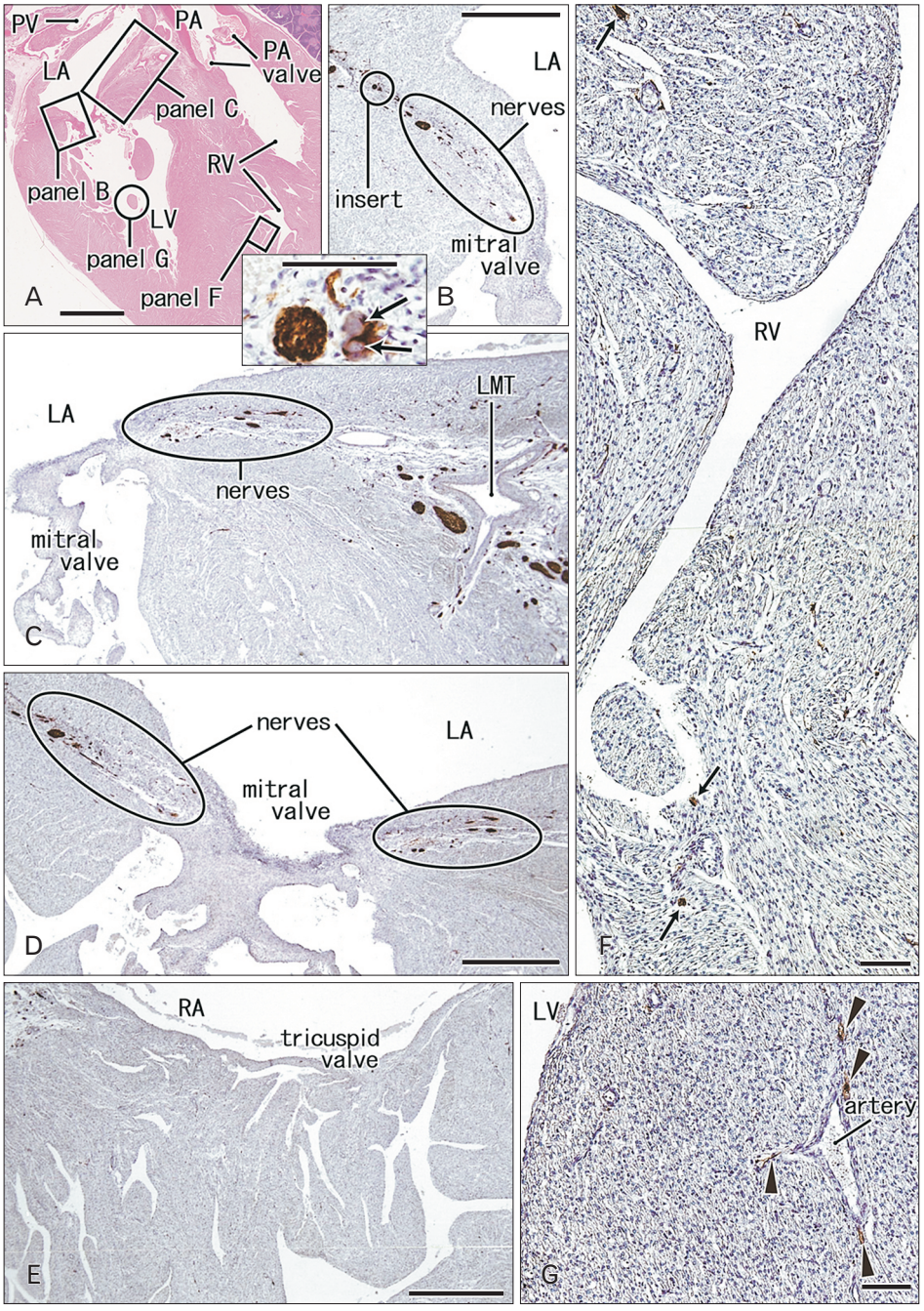

Fig. 5. Nerves and ganglia around the atrioventricular valves and in ventricular muscles of the heart. 31 weeks. Sagittal sections through the outflow tract of the right ventricle (RV) and the mitral valve of the left ventricle (LV). Hematoxylin and eosin staining (A) and immunostaining of S100 protein (B–G). Squares in panel A are shown in panels B, C, F and G at the higher magnification. Panels B–D display nerves around the mitral valve annulus. Panel D shows a plane 0.5 mm left side of panel C. An insert between panels A and B displays ganglion cells (arrows) near the base of the mitral valve. Panel E exhibits the tricuspid valve of the same specimen (corresponding to a square in Fig. 4A). In contrast to abundant nerves around the mitral valve annulus (B–D), few nerves are seen around the tricuspid valve annulus (E). Panel F shows muscular nerves (arrows) in trabeculae of the RV: parts of them are exposed to the expanding ventricular endothelium. Panel G displays a nerve net (arrowheads) along an artery in the papillary muscle of the LV. LA, left atrium; LMT, left main trunk of the coronary artery; PA, pulmonary artery; PV, pulmonary vein; RA, right atrium. Scale bars=5 mm (A), 1 mm (B–E), 0.1 mm (F, G, insert between A and B).

https://doi.org/10.5115/acb.2019.52.1.48

sections with 50-μm interval, numbers of ganglion cell bodies ranged from 170 to 250 between the ascending aorta and pulmonary trunk, 150–200 at and near the crux and 30–150 in front of the pulmonary trunk.

The left common cardinal vein had lost the vascular lumen near the posterior body wall due to degeneration. This vein accompanied abundant nerves in and outside of the atrioventricular sulcus (Figs. 1F, 6B). These nerves came from an extracardiac nerve plexus between the left primary bronchus and pulmonary artery (Fig. 1A) via a narrow space between the left pulmonary vein and left atrium (Fig. 1C, D). They were likely to correspond to the left and middle dorsal subplexuses of Pauza et al [1]. Likewise, abundant nerves were also evident along the left superior pulmonary vein as well as a site between the vein and left atria (Fig. 2C, D): the vein and atria made a thick and wide fold corresponding to the left atrial nerve fold (see the first paragraph of the Introduction). These nerves appeared to correspond to the ventral left atrial subplexus and/or the left dorsal subplexus of Pauza et al. [1]. Most nerves to the left atrial nerve fold came from an extra-

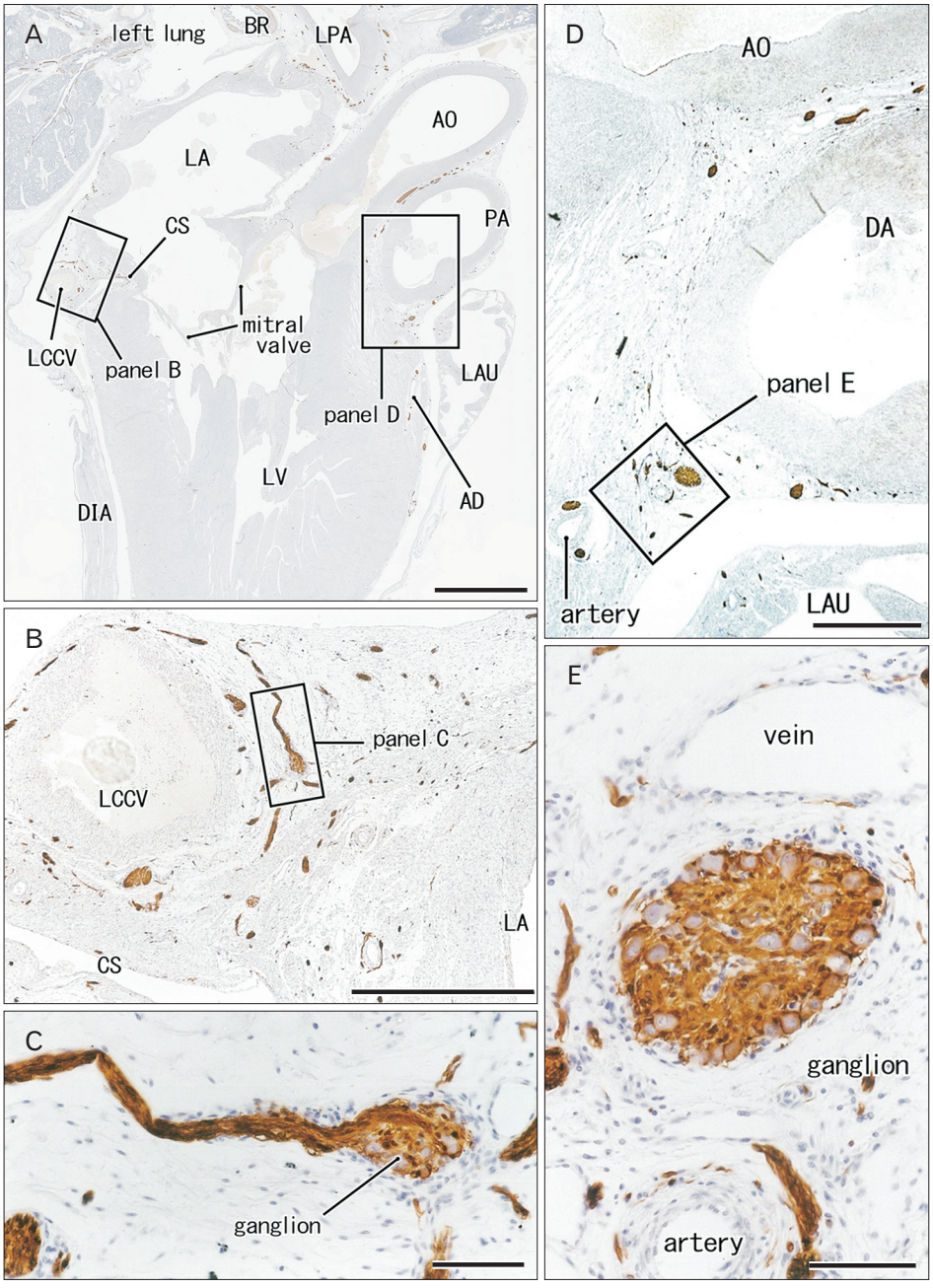

Fig. 6. Nerves and ganglia along the coronary sulcus of the heart. 30 weeks. Sagittal section through the aortic outflow tract of the left ventricle (LV) as well as the mitral valve. Immunostaining of S100 protein. Two squares in panel A are shown in panels B and D at the higher magnification. A ganglion in panel B or D is shown in panel C or D at the higher magnification. The left common cardinal vein (LCCV) is degenerating and obliterated in a plane 3 mm left of panel B, but it accompanies abundant nerves (B). AD, anterior descending branch of the left coronary artery; AO, aorta; BR, bronchus; CS, coronary sinus; DA, ductus arteriosus; DIA, diaphragm; LA, left atrium; LAU, left auricle; LPA, left pulmonary artery; PA, pulmonary artery. Scale bars=5 mm (A), 1 mm (B, D), 0.1 mm (C, E).

cardiac nerve plexus under the aortic arch as well as between the arch and ductus arteriosus (Fig. 2A). This nerve origin usually contained a large ganglion (ganglion cardiacum) near the origin of the left recurrent laryngeal nerve.

In the ventricular myocardium including the atrioventricular junction and interventricular septum, nerves were distributed deeply and seen with or without vessels accompanied (Figs. 2B, 3B, 5G). Notably, a high density of nerves was consistently evident around the mitral valve annulus, whereas the tricuspid valve annulus accompanied much less numbers of nerves (Fig. 5C–E). As ventricular myocardium was degenerated in the luminal side for sculpturing of papillary muscles and trabeculae, nerves near the ventricular cavity became exposed to the ventricular cavity (Figs. 2E, 4B, 5F). Likewise, as pectineal muscles were sculptured, nerves were exposed in the atrial cavity (Fig. 3H). Sometimes (3 specimens), we found thin nerves running along a long distance (0.5–1.0 mm) beneath the atrial endothelium (Figs. 3D, 4C).

In the posterosuperior and left sides of the oval foramen, the primary septum was attached tightly to the secondary septum. The attaching or fusion of the septa varied between specimens in area. The upper tip of the primary septum appeared to be a thin fold or valve arising from the original septum (Fig. 4C). The valve of the oval foramen carried no nerves and vessels. Notably, the primary septum contained few nerves and no vessels, whereas the secondary septum had abundant nerves and vessels (Figs. 3E, 4D, F). The myocardium along and near the coronary sinus and inferior caval orifice contained abundant nerves and ganglion cells (Figs. 3C, F, G, 4D, E).

Discussion

The most striking feature in the present study was found in the luminal aspects of the ventricular and atrial wall: early-developed nerves became exposed to the ventricular or atrial endothelium due to sculptured myocardium during development of papillary muscles, pectinate muscles and trabeculae. Remodeling of myocardium occurs after midterm [16], partly involves cell death [17] and regulated by bone morphogenetic protein 4 (BMP4) and fibroblast growth factor 2 (FGF2) [18]. The latter group demonstrated that, *in vitro*, BMP4 induces, whereas FGF2 inhibits, apoptosis of mouse embryonic ventricular myocardium. The process to provide papillary and pectinate muscles was previously termed "luminal trabeculation" and recently called "myocardial assembly" [19]. Possibly due to unbalance between luminal expansion and myocardial growth, parachute-like asymmetric growth occurs for development of papillary muscles [20]. Therefore, conversely, early nerve growth in the myocardium seemed to be out of the regulation for myocardial assembly.

We found another striking feature in the growing atrial septum: the secondary septum contained abundant thick nerves in contrast to no or few nerves in the primary septum. This difference was most evident at the left posterior margin of the oval foramen in which these two septa are attached tightly. Singh et al. [21] found several ganglion cells in the adult atrial septum, but we did not in fetuses. Thus, the postnatal development of ganglion cells seemed to be likely in the atrial septum. We also found a clear difference in nerve density between the mitral and tricuspid annuluses: a high density of nerves around the mitral valve in contrast to few nerves around the tricuspid valve. This difference might be connected with arrhythmia after replacement surgery of these valves. However, a patient requiring tricuspid valve replacement is usually suffering from a combination of anomalies such as Ebstein's anomaly [22, 23]. Thus, it seemed to be difficult to compare between clinical outcomes of the mitral and tricuspid valve surgeries

According to our recent study [24], epicardiac nerves and ganglion cells along the left common cardinal vein are quite different from those at the origins of the great arteries in proportion of tyrosine hydroxylase (TH)- and neuronal nitric oxide synthase (nNOS)-positive neurons. The present observations suggested that, depending on expansion of the left atrium, the nerves along the left common cardinal vein were likely to be involved in the atrial-pulmonary vein junction. Likewise, nerves in the left atrial nerve fold were also likely to supply the atrial-pulmonary vein junction because the growing fold made the atrium and vein more separated. These nerves came from the ganglion cardiacum and this ganglion contains abundant TH-positive neurons and a few nNOS-positive neurons. Therefore, nerves to the atrial-pulmonary vein junction seemed to have dual origins and fiber components. Pauza et al. [1] considered that the left atrial fold nerve is originated from nerves passing through the venous pole of the heart: this was not contradict to the present observations since parts of the composite nerve fibers came along the left common cardinal vein. The atrial-pulmonary vein junction is likely to contain a histopathological substrate of chronic atrial fibrillation: the pathological difference in substrate is likely to be found in phenotypes of neurons [4, 5, 7], but the

https://doi.org/10.5115/acb.2019.52.1.48

other researchers considered it simply as a difference in nerve density [6, 25]. A proportion between the dual nerve origins in fetuses might be connected with an individual difference in histological substrate.

Acknowledgements

This study was supported by Grant-in-Aid (Grant number: JSPS KAKENHI NO. 16K08435) for Scientific Research from the Ministry of Education, Culture, Sports, Science and Technology in Japan.

References

1. Pauza DH, Skripka V, Pauziene N, Stropus R. Morphology, distribution, and variability of the epicardiac neural ganglionated subplexuses in the human heart. Anat Rec 2000;259:353-82.
2. Worobiew W. Plica nervina atrii sinistri. Z Anat Entwicklungsgesch 1928;86:509-16.
3. Gardner E, O'Rahilly R. The nerve supply and conducting system of the human heart at the end of the embryonic period proper. J Anat 1976;121:571-87.
4. Tan AY, Li H, Wachsmann-Hogiu S, Chen LS, Chen PS, Fishbein MC. Autonomic innervation and segmental muscular disconnections at the human pulmonary vein-atrial junction: implications for catheter ablation of atrial-pulmonary vein junction. J Am Coll Cardiol 2006;48:132-43.
5. Nguyen BL, Fishbein MC, Chen LS, Chen PS, Masroor S. Histopathological substrate for chronic atrial fibrillation in humans. Heart Rhythm 2009;6:454-60.
6. Deneke T, Chaar H, de Groot JR, Wilde AA, Lawo T, Mundig J, Bösche L, Mügge A, Grewe PH. Shift in the pattern of autonomic atrial innervation in subjects with persistent atrial fibrillation. Heart Rhythm 2011;8:1357-63.
7. Matsuyama TA, Tanaka H, Adachi T, Jiang Y, Ishibashi-Ueda H, Takamatsu T. Intrinsic left atrial histoanatomy as the basis for reentrant excitation causing atrial fibrillation/flutter in rats. Heart Rhythm 2013;10:1342-8.
8. Marron K, Wharton J, Sheppard MN, Fagan D, Royston D, Kuhn DM, de Leval MR, Whitehead BF, Anderson RH, Polak JM. Distribution, morphology, and neurochemistry of endocardial and epicardial nerve terminal arborizations in the human heart. Circulation 1995;92:2343-51.
9. Armour JA, Murphy DA, Yuan BX, Macdonald S, Hopkins DA. Gross and microscopic anatomy of the human intrinsic cardiac nervous system. Anat Rec 1997;247:289-98.
10. Singh S, Johnson PI, Javed A, Gray TS, Lonchyna VA, Wurster RD. Monoamine- and histamine-synthesizing enzymes and neurotransmitters within neurons of adult human cardiac ganglia. Circulation 1999;99:411-9.
11. Singh S, Gray T, Wurster RD. Nitric oxide and carbon monoxide synthesizing enzymes and soluble guanylyl cyclase within neurons of adult human cardiac ganglia. Auton Neurosci 2009;145:93-8.
12. Hoover DB, Isaacs ER, Jacques F, Hoard JL, Pagé P, Armour JA. Localization of multiple neurotransmitters in surgically derived specimens of human atrial ganglia. Neuroscience 2009;164:1170-9.
13. Taguchi K, Tsukamoto T, Murakami G. Anatomical studies of the autonomic nervous system in the human pelvis by the whole-mount staining method: left-right communicating nerves between bilateral pelvic plexuses. J Urol 1999;161:320-5.
14. Orts Llorca F, Domenech Mateu JM, Puerta Fonolla J. Innervation of the sinu-atrial node and neighbouring regions in two human embryos. J Anat 1979;128:365-75.
15. Hachisuka H, Mori O, Sakamoto F, Sasai Y, Nomura H. Immunohistological demonstration of S-100 protein in the cutaneous nervous system. Anat Rec 1984;210:639-46.
16. Captur G, Wilson R, Bennett MF, Luxán G, Nasis A, de la Pompa JL, Moon JC, Mohun TJ. Morphogenesis of myocardial trabeculae in the mouse embryo. J Anat 2016;229:314-25.
17. Cheng G, Wessels A, Gourdie RG, Thompson RP. Spatiotemporal and tissue specific distribution of apoptosis in the developing chick heart. Dev Dyn 2002;223:119-33.
18. Zhao Z, Rivkees SA. Programmed cell death in the developing heart: regulation by BMP4 and FGF2. Dev Dyn 2000;217:388-400.
19. Sedmera D, Pexieder T, Vuillemin M, Thompson RP, Anderson RH. Developmental patterning of the myocardium. Anat Rec 2000;258:319-37.
20. Oosthoek PW, Wenink AC, Wisse LJ, Gittenberger-de Groot AC. Development of the papillary muscles of the mitral valve: morphogenetic background of parachute-like asymmetric mitral valves and other mitral valve anomalies. J Thorac Cardiovasc Surg 1998;116:36-46.
21. Singh S, Johnson PI, Lee RE, Orfei E, Lonchyna VA, Sullivan HJ, Montoya A, Tran H, Wehrmacher WH, Wurster RD. Topography of cardiac ganglia in the adult human heart. J Thorac Cardiovasc Surg 1996;112:943-53.
22. Pasque M, Williams WG, Coles JG, Trusler GA, Freedom RM. Tricuspid valve replacement in children. Ann Thorac Surg 1987;44:164-8.
23. Ross FJ, Latham GJ, Richards M, Geiduschek J, Thompson D, Joffe D. Perioperative and anesthetic considerations in Ebstein's anomaly. Semin Cardiothorac Vasc Anesth 2016;20:82-92.
24. Kim JH, Cho KH, Jin ZW, Murakami G, Abe H, Chai OH. Ganglion cardiacum or juxtaductal body of human fetuses. Anat Cell Biol 2018;51:266-73.
25. Zhao QY, Huang H, Zhang SD, Tang YH, Wang X, Zhang YG, Salim M, Okello E, Deng HP, Yu SB, Huang CX. Atrial autonomic innervation remodelling and atrial fibrillation inducibility after epicardial ganglionic plexi ablation. Europace 2010;12:805-10.